Biochimica et Biophysica Acta 436, (1976) 307–318

BBA 77335

MULTIPLE THERMOTROPIC STATE TRANSITIONS IN ERYTHROCYTE MEMBRANES

A LASER-RAMAN STUDY OF THE CH-STRETCHING AND ACOUSTICAL REGIONS

SURENDRA P. VERMA and DONALD F. H. WALLACH

Division of Radiobiology, Department of Therapeutic Radiology, Tufts-New England Medical Center, 171 Harrison Avenue, Boston, Mass. 02111 (U.S.A.)

(Received November 25th, 1975)

SUMMARY

1. We have examined the Raman scattering from erythrocyte ghosts at 2700 cm^{-1}–3000 cm^{-1} (CH-stretching region), that at low frequencies due to acoustical vibrations, as well as that due to ν (–C=C–) and ν (=C–C=) of β-carotene, in the temperature range of −30 °C to +30 °C. For comparison we have also evaluated the Raman spectra of liposomes composed of lecithins±cholesterol.

2. Plots vs. temperature of the intensities (I) of the approx. 2880 cm^{-1} and 2932 cm^{-1} bands relative to the intensity of the thermally stable 2850 cm^{-1} band, i.e. the $[I_{2880}/I_{2850}]$ and $[I_{2932}/I_{2850}]$ ratios, reveal discontinuities in both erythrocyte membranes and liposomes.

3. In erythrocyte membranes, plots of $[I_{\approx 2880}/I_{2850}]$ and $[I_{\approx 2932}/I_{2850}]$ reveal several discontinuities. Those reported by $[I_{\approx 2880}/I_{2850}]$ occur at +17 °C and approx. −4 °C. The ratio $[I_{\approx 2932}/I_{2850}]$ reveals a transition between −20 °C and +10 °C, 1/2 maximal at −8 °C. The ratio $[I_{1527}/I_{1158}]$, representing the relative intensity of ν (–C=C–) vs. ν (=C–C=) of membrane-bound β-carotene, changes discontinuously with the 17 °C transition, but is stable over the rest of the temperature range studied.

4. The data indicate that a major membrane-state transition takes place below 0 °C but that an additional transition occurs at approx. 17 °C.

INTRODUCTION

The plasma membranes of erythrocytes [1–3], thymocytes [4, 5] and other lymphoid cells [6] exhibit well resolved Raman spectra which yield insights into the structures of membrane lipids and proteins, as well as into the interactions between these components. In addition, Raman spectroscopy has provided important information about thermotropic state transitions in model lipid membranes [4, 7–9] as well in thymocyte plasma membranes [4]. The latter exhibit a thermotropic lipid state transition (near 23 °C), that is revealed by the variation of CH-stretching scattering with temperature.

We now report on the thermotropism of erythrocyte membranes as revealed by the variation with temperature of Raman scattering in the CH-stretching region and of low-frequency acoustical vibrations [10, 11], as well as of resonance-enhanced scattering due to the –C=C– and =C–C= stretching vibrations of membrane-bound β-carotene [1, 2].

Our survey of the low frequency spectral regions demonstrates the utility of Raman spectroscopy in evaluating the ordering of apolar domains of model and biomembranes. In addition, our experiments reveal a complex thermal response of erythrocyte membrane hydrocarbon residues. This is interpreted in terms of the thermal behavior of lecithin liposomes, of liposomes composed of lecithin plus cholesterol, lecithin plus β-carotene and lecithin plus melittin (a small ampipathic polypeptide that interacts hydrophobically with phosphatide acyl chains) [7], [12], as well as of mixed lipid systems containing charged phosphatides [13].

EXPERIMENTAL

Chemicals. Egg lecithin, lysolecithin and lysophosphatidylethanolamine were obtained from Lipid Products (South Nutfield, U.K.); palmitoylcholine chloride, from Serdary Research Laboratories (London, Ontario, Canada); cholesterol, β-carotene, phosphorylethanolamine and phosphorylcholine from Sigma, (St. Louis, Mo., U.S.A.). All other reagents were of analytical grade.

Membranes. Erythrocyte ghosts were prepared at pH 7.4 according to the method of Fairbanks et al. [14] from freshly drawn, heparinized blood, resuspended in 5 mM phosphate, pH 7.4, pelleted at $6 \cdot 10^6 \times g_{av}$ per min, using a Spinco ultracentrifuge (L265B; Rotor SW56), resuspended in 5 mM phosphate, pH 7.4 sonicated for 20 s at 20 °C, (Sonic Dismembranator, Quigley-Rochester, Rochester, N.Y.; power step 30), pelleted at $1.2 \cdot 10^7 \times g$ per min and resuspended in 0.1 ml 5 mM phosphate, pH 7.4, at a concentration of approx. 10 mg protein/ml.

Liposomes. Lecithin liposomes (40 mg/ml, ±additives at stated ratios) were prepared by the method of other authors [1, 2, 4–6] by sonication at 4 °C (power step 3).

Raman spectroscopy. Membrane vesicles and liposomes were transferred to 1.6–1.8 mm internal diameter Kimex Capillaries. After sealing, the sample capillaries were placed in a Harney-Miller Cell [15] for temperature control. The temperature was monitored by a telethermometer and regulated by a flow of nitrogen. Temperature control was checked by determining transition temperatures of authentic lipids (dimyristoylphosphatidylcholine; dipalmitoylphosphatidylcholine) in the laser beam.

Raman spectra were recorded as before [1, 2, 4–7] using a Ramalog 4 Raman spectrometer (Spex Industries, Metuchen, N.J., U.S.A.) interfaced to an Interdata (Model 70) computer. An Ar^+ laser (Spectra Physics model 164), tuned at 488 nm, was used as an excitation source. For spectra at low frequencies an interference filter was used to block out plasma lines. Power was 300 mW, except for β-carotene resonance Raman spectroscopy, where 50 mW was used. The Raman scattering at right angles to the laser beam was detected by a thermoelectrically-cooled photomultiplier (RCA 31034) and was recorded in terms of photons/s. The "dark" rates of the photo cell were < 50 counts/s. Raman scattering from the sample gave rates in the order of 10^3–10^5/s. Scanning was done through the computer (loaded with the

VIE8D Ramacomp Computer Program, Spex Industries). The specifications for scanning: maximum time and minimum time for each data point were 1 s and 0.5 s respectively, except for the β-carotene lines, where we used 0.5 s and 0.1 s respectively. The photon counts were 10^4–10^5 maximum and 100 minimum. Scanning was in steps of one wave number. Scans were incremental between data points and no counts were recorded between data points. Photon counts were stored in the computer memory during scanning (2–4 scans) and the stored spectra, averaged and smoothed by a least squares procedure; (included in the computer program) [16], were ultimately plotted on the Ramalog recorder, using appropriate background suppressions and scale expansions. To accurately determine the positions of some low-frequency bands, first- and second-derivative spectra were computed and recorded.

To determine the change of Raman scattering with temperature we proceeded as follows: the samples, in position but with the laser beam occluded, were equilibrated for 20 min at the desired temperature. For CH-stretching scattering the samples were then equilibrated a further 5 min in the laser beam before scanning from 2750 cm^{-1} to 3050 cm^{-1} (2–4 scans; maximum 300 s/scan). During equilibration at the subsequent temperature the averaged, smoothed spectra were plotted. The procedure for the 1527 cm^{-1} and 1158 cm^{-1} bands of β-carotene was identical except that the 5 min equilibration in the laser beam was omitted and scanning was from 1400 cm^{-1}–1600 cm^{-1} and 1000 cm^{-1}–1200 cm^{-1} respectively (maximum 100 s/scan for each band).

Scattering vs. temperature curves were similar whether proceeding from high to low temperatures or vice versa. All experiments were carried out on at least three separate membrane preparations (erythrocyte membranes or liposomes) and intensity ratios are given as means $\pm$ practical error.

The thermal responses of intact ghosts did not differ significantly from those of the sonicated membranes; but, the latter were preferred because they yield higher membrane concentrations.

RESULTS AND DISCUSSION

CH-stretching region

The intense bands in membranes at 2850 cm^{-1} and 2880 cm^{-1} (Fig. 1) have been assigned to symmetric and asymmetric CH-stretching, respectively, of methylene groups [7, 9, 17–19]. The other major band at 2930 cm^{-1}–2940 cm^{-1} (Fig. 1) have been thought to include contributions due to asymmetric CH-stretching from methylenes in short segments [4, 19] as well as symmetric CH-stretching from amino acid side chain CH_3 groups and from terminal CH_3 residues of lipid acyl chains.

The Raman scattering bands in the CH-stretching region change markedly as the temperature is varied between -30 °C and $+30$ °C (Fig. 1), with much narrower line widths occurring at temperatures below -20 °C. Importantly, the intensities of the 2880 cm^{-1}–2890 cm^{-1} band and the 2930 cm^{-1}–2940 cm^{-1} band relative to the intensity of the 2850 cm^{-1} peak, i.e. the $[I_{\approx 2880}/I_{2850}]$ and $[I_{\approx 2932}/I_{2850}]$ ratios, respectively, change discontinuously with temperature (Fig. 2) revealing at least two distinct thermotropic events. $[I_{\approx 2932}/I_{2850}]$ rises from a value of 0.83 ± 0.12, stable below -20 °C, to a value of 1.15 ± 0.17, stable to $+30$ °C, with a half-maximal change at -8 °C. In contrast, the variation of $[I_{\approx 2880}/I_{2850}]$ with temperature is

biphasic. The first decrement is asymmetric. It begins below −20 °C (1.56±0.10) and extends to approx. +4 °C (1.17±0.05). It is half maximal below −3 °C and approximately follows the $[I_{\approx 2932}/I_{2850}]$ transition. The second step, from 1.15± 0.05 to 1.00±0.03, occurs between 14 °C and 20 °C (1/2 maximal at 15 °C). If we

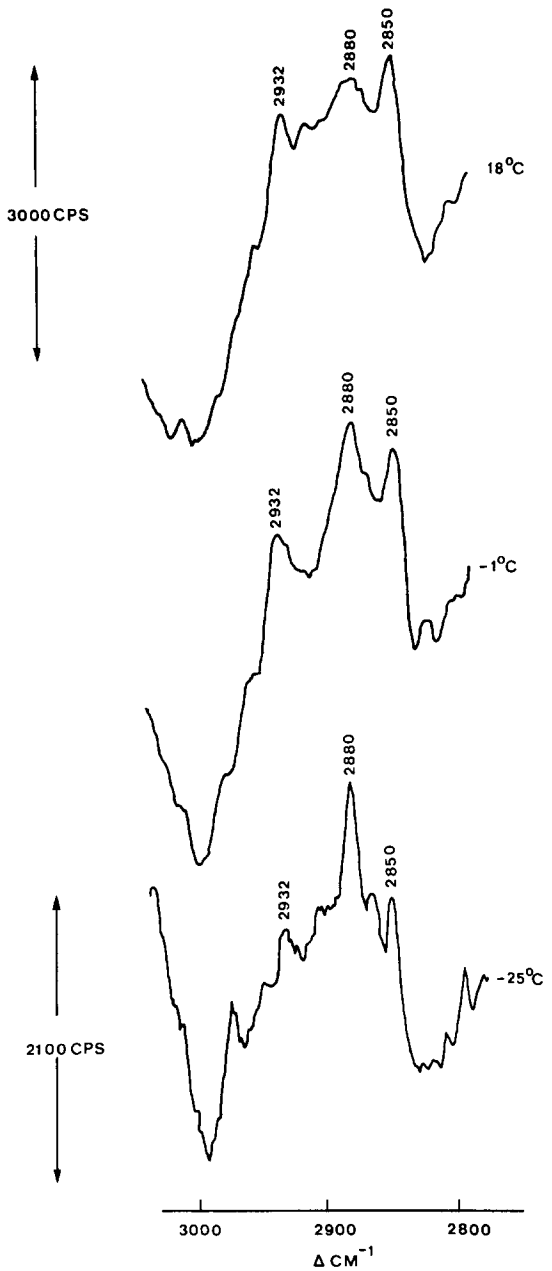

Fig. 1. Raman spectra, in the CH-stretching region, of erythrocyte membranes at several temperatures. Exciting wavelength 488 nm. Power 300 mW. Resolution 5 cm^{-1}.

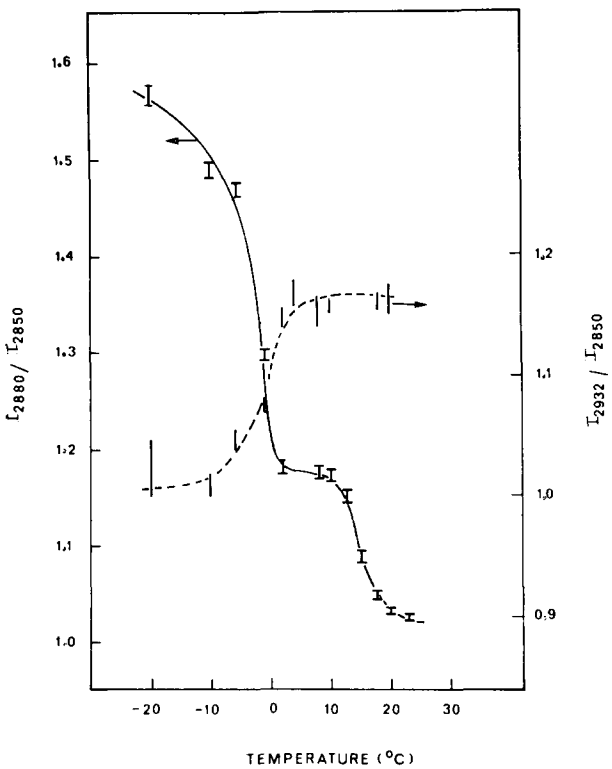

Fig. 2. Variation with temperature of $[I_{\approx 2880}/I_{2850}]$ (left ordinate) and $[I_{2932}/I_{2850}]$. (right ordinate) of erythrocyte membranes. ———, $[I_{2880}/I_{2850}]$; – – – –, $[I_{2932}/I_{2850}]$. The bars give ranges of experimental values.

correct for the local heating due to the laser beam we arrive at the following "transition" temperatures: −8 °C ($[I_{\approx 2932}/I_{2850}]$), below −4 °C, (first step in $[I_{\approx 2880}/I_{2850}]$) and +17 °C (second $[I_{\approx 2880}/I_{2850}]$ step).

β-Carotene signals

The second decrement in $[I_{\approx 2880}/I_{2850}]$ is associated with a change of $[I_{1527}/I_{1158}]$ from 1.3–1.4 to 1.0–1.1. In contrast, $[I_{1527}/I_{1158}]$ does not change between −30 °C and +14 °C. This suggests that the β-carotene in erythrocyte membranes is restricted to the lipid domain undergoing a state of transition between 14 °C and 20 °C. The direction of change of $[I_{1527}/I_{1158}]$ in this temperature range corresponds to that accompanying gel → liquid-crystal transitions in lecithin liposomes doped with β-carotene [7].

Acoustical region (400 cm^{-1}–100 cm^{-1})

The C–C chain acoustical modes of phospholipid acyl chains occur in this region [10, 11] and, since they depend on whether the chains are in a crystalline array or not, can be expected to reflect the order of phospholipid acyl chains in model and bio-membranes under diverse conditions. The low frequency region is also expected to include vibrations from other crystalline domains [20].

TABLE I

LOW FREQUENCY RAMAN SCATTERING BY VARIOUS PHOSPHORYLATED COMPOUNDS

H_3PO_4	NaH_2PO_4		Na_2HPO_4		Phosphoryl-choline	Phosphoryl-ethanolamine	Tentative assignment
(80%)	crystal	solution	crystal	solution	crystal	crystal	
			425				
	418						
		396	400	396		415	Phosphate-deformation
380	379	370	380	380	370	360	
360	295		310		308	295	
	260		255		255	250	Phosphate lattice modes
	228		230		230		
	190		190		192	195	Phosphate lattice modes

Model compounds. Crystalline NaH_2PO_4 yields bands at 418, 379, 295, 260, 228 and 190 cm^{-1}, whereas crystalline Na_2HPO_4 gives bands at 425, 400, 380, 310, 255, 230 and 190 cm^{-1}. (Table I). Crystalline phosphorylcholine and phosphorylethanolamine yield bands at 370, 308, 255, 230, 192 and 415, 360, 295, 250 and 195 cm^{-1}, respectively (Table I). None of these bands, except those at approx. 400 cm^{-1} and at 370–360 cm^{-1}, are observed with saturated aqueous solutions of the listed compounds (also, 80 % phosphoric acid exhibits bands only at 380 cm^{-1} and 360 cm^{-1}). The bands of the crystalline solids at frequencies below 300 cm^{-1} may represent phosphate lattice modes. The peaks at higher frequencies, apparent also in aqueous solutions may represent phosphate deformation vibrations.

Crystalline palmitoyl choline yields distinct bands at 340 cm^{-1} and at 160 cm^{-1}. The latter is a characteristic C–C acoustical vibration of the C_{16} palmitate chain [10]. Glycerol exhibits a strong band at approx. 330 cm^{-1}.

Lecithin liposomes. Fig. 3 and Table II present important low-frequency features of egg lecithin liposomes when the phospholipid is in the liquid-crystal phase (18 °C) and in the crystal state (−11 °C).

The approx. 365 cm^{-1} peak, 350 cm^{-1} shoulder and 290 cm^{-1} band at 18 °C, presumably due to phosphate deformations, shift into sharp bands at 370 cm^{-1}, 350 cm^{-1} and 310 cm^{-1}. The asymmetrical band peaking at 260 cm^{-1} (not seen in chloroform solutions of lecithin) persists to approx. −5 °C but at lower temperatures shifts into a shoulder of a strong band at 245 cm^{-1}. The band at 195 cm^{-1} (also not seen in chloroform solution) disappears below the transition temperature. We cannot now provide assignment for these bands. The shoulder at 150–170 cm^{-1}, seen at all temperatures above freezing is due to hindered translation (ν_T) in liquid water [21]*. Upon freezing, which here occurs between −1 °C and −2 °C, due to supercooling, the strong ν_t band of Ice I appears at 215 cm^{-1}. As expected [21], this band shifts to higher frequencies with decreasing temperature. It lies at 218 cm^{-1} at −30 °C and probably corresponds to the 218 cm^{-1} band, previously attributed to crystalline oleate in aqueous sonicates of dioleoyllecithin at −62 °C [10].

* The frequency position of this varies inversely with temperature between −5 °C and 95 °C [21].

The strong band which appears near 245 cm^{-1} in the crystalline state is attributable to the oleate chain of the lecithin.

By comparing the second derivatives of the liposome spectra with those of water, the deformity in the low frequency limb of the 210 cm^{-1} Ice I band (Fig. 3) is shown to arise from a band at 208 cm^{-1}; this can also be attributed to the oleate chains [10]. The feature at 160 cm^{-1} includes contributions from both palmitate and oleate chains, as well as from water (Fig. 3).

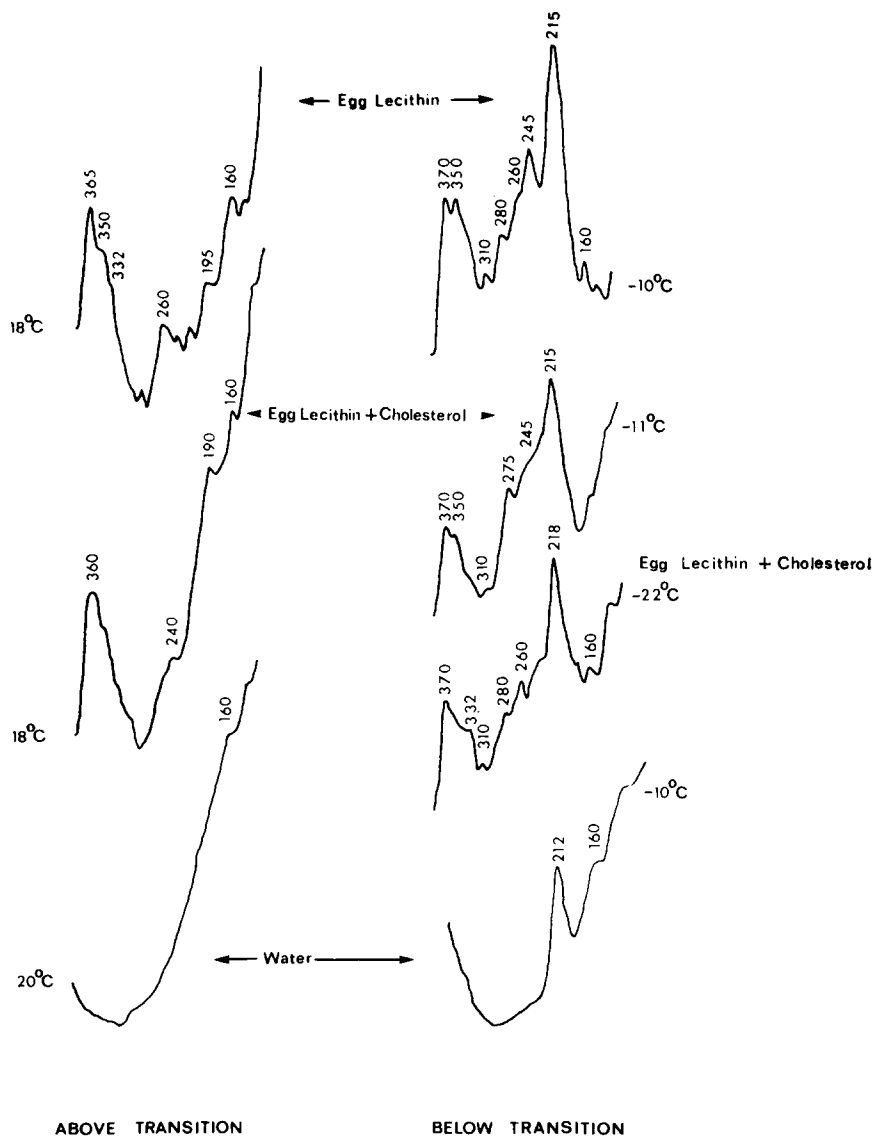

Fig. 3. Raman spectra in the acoustical region of egg lecithin, egg lecithin/cholesterol liposomes, and water above and below the egg lecithin transition temperature.

TABLE II

LOW FREQUENCY RAMAN SCATTERING BY EGG LECITHIN LIPOSOMES AT VARIOUS TEMPERATURES

38 °C	25 °C	20 °C	18 °C	16 °C	7 °C	5 °C	−10 °C	Tentative assignment
370	360	360	367	370	365	370	370	Phosphate deformation
335	340	340	350	350	350	347	353	Glycerol
310	310	300	290	300	290	312	310	
						285	285	
260	260	255	260	258	260	250	260	
							245	Unsaturated chain, crystalline; acoustical
	190	190	190			185		
	160	160	160	160	160	160	165	Fatty acid chain, crystalline; acoustical

Lecithin/cholesterol liposomes. As shown in Fig. 3, (Table II), lecithin/cholesterol liposomes (1 mol cholesterol per mol of phospholipid) exhibit different low-frequency spectra from sterol-free liposomes both above and below the lecithin transition temperature (−5.5 °C). Prominent above the transition temperature is the lack of the 260 cm^{-1} band; there is only a weak shoulder at approx. 240 cm^{-1}. At −11 °C the lecithin/cholesterol spectrum differs from the corresponding lecithin spectrum in that the prominent 245 cm^{-1} band (attributed to oleate) is reduced to a broad shoulder. The 245 cm^{-1} band does not resolve even at −22 °C, although the 260 cm^{-1} band does emerge at that temperature (Fig. 3).

The results suggest that above the transition temperature, the presence of cholesterol perturbs the lattice structure of lecithin headgroups. Below the lecithin transition temperature the sterol impedes the ordering of acyl chains (cf. lacking 245 cm^{-1} band). This is what is expected from the established behavior of cholesterol [22].

Erythrocyte membranes. The acoustical region of erythrocyte membranes at several temperatures is represented in Fig. 4. The spectrum at +2 °C resembles those obtained at higher temperatures and is remarkable for its lack of detail compared with the spectrum of lecithin liposomes and even cholesterol/lecithin liposomes. At −1 °C shoulders emerge at 255, 232 and 210 cm^{-1}. These may reflect crystallization of unsaturated chains, which, according to the changes in the CH-stretching region should be in progress at this temperature. In the −6 °C spectrum the region between 230 cm^{-1} and 190 cm^{-1} is obscured by the Ice I peak, but there is no indication of any structuring at frequencies expected of the acoustical modes of unsaturated or saturated acyl chains. However, some detail does emerge at −25 °C with bands at 318 cm^{-1}, 298 cm^{-1}, 280 cm^{-1} a sharp shoulder at 260 cm^{-1} and a weak shoulder at approx. 193 cm^{-1}. The behavior of the erythrocyte-membranes thus resembles that of lecithin/cholesterol liposomes and may derive at least in part from their high cholesterol content.

GENERAL DISCUSSION

Erythrocyte membranes exhibit no thermotropic lipid phase transitions that can be detected by differential thermal calorimetry [23] or X-ray analyses [24]. Also, erythrocyte membrane proteins lack significant mobility in the plane of the mem-

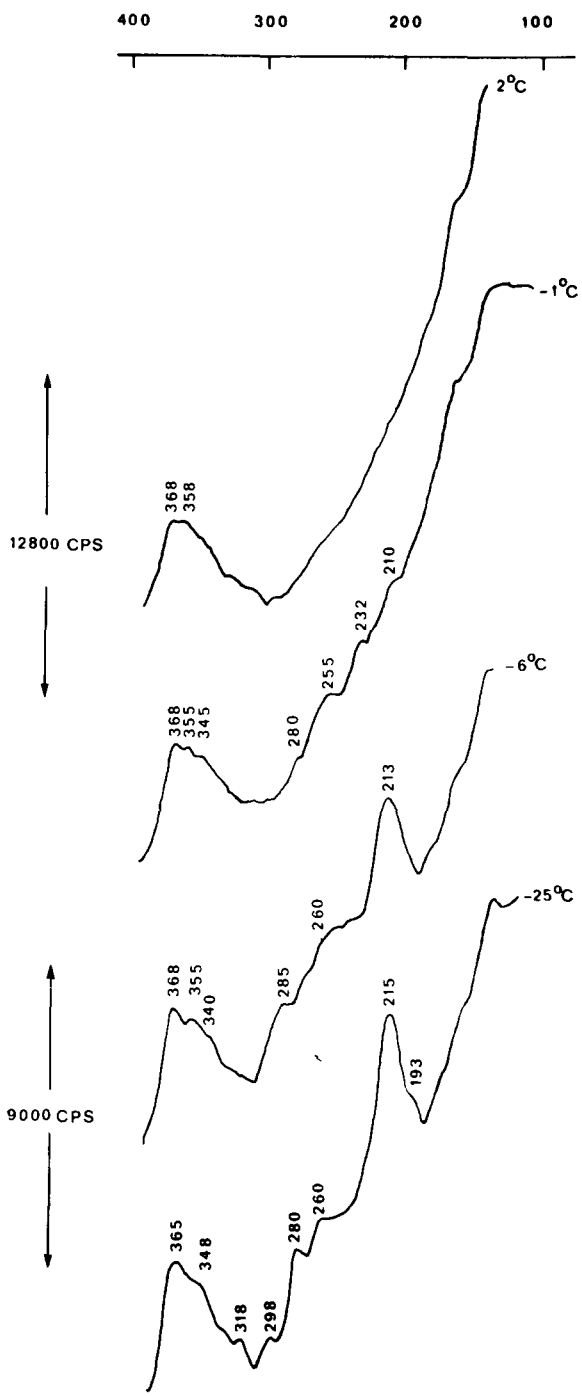

Fig. 4. Raman spectra in the acoustical region of erythrocyte membranes at various temperatures.

brane [25] and appear to exert considerable constraint on the mobilities of membrane lipids, as measured by use of spin-labelled probes [26, 27]. Moreover, X-ray analyses of erythrocyte membrane-lipid liposomes that are not excessively depleted of cholesterol, show a liquid-crystal state exclusively even at −20 °C. However, Zimmer and associates [28, 29] describe a thermotropic viscosity change, discontinuous at 18–20 °C, in erythrocyte membranes, as well as cholesterol-depleted membrane lipids and have related this to the discontinuity at 19 °C in the Arrhenius plot for glucose transport [30].

One explanation for these apparently inconsistent observations is that the diverse experimental approaches used monitor different properties of a composite membrane. Evidence in support of this notion is already in hand. Thus, Raman spectroscopy reveals thermotropic gel → liquid-crystal transitions in lecithin/cholesterol mixtures [7, 8] that are not detected by differential thermal calorimetry. Similarly, Raman studies demonstrate a cooperative, thermotropic lipid state transition in thymocyte plasma membranes despite their high cholesterol content [4]. Also, several studies [26–32] clearly suggest a restrained organization of lipids and proteins in erythrocyte membranes. Indeed, recent experimentation, [31, 32] using nitroxide-labelled lipid analogues to paramagnetically quench the tryphophan fluorescence of membrane proteins suggest that erythrocyte membranes contain both cholesterol-depleted boundary layers of phospholipid abutting membrane proteins, relatively fluid phosphatide domains of low cholesterol content, as well as cholesterol clusters. There is also electron microscopic evidence for cholesterol clustering in erythrocyte membranes [33].

Our studies reveal at least two thermotropic state transitions when erythrocyte membranes are cycled between −30 °C and +25 °C. That below 4 °C can be ascribed at least in part to disorder $\rightleftarrows$ order transitions of membrane lipid chains, because of the thermal changes in the acoustical region. However, we cannot now unambiguously assign the origins of the thermotropism in the CH-stretching region.

First, as pointed out by Lord (Lord, R. C., personal communication), CH-stretching vibrations should not be thermally sensitive and the thermotropism of $[I_{\approx 2880}/I_{2850}]$, as well as $[I_{\approx 2932}/I_{2850}]$ might derive from overtones (enhanced by Fermi resonance) [34] of the environmentally-sensitive HCH deformations (with fundamentals near 1440 cm^{-1}–1465 cm^{-1}; e.g. ref. 10).

Second, we cannot be certain to what extent the thermally induced changes derive from lipid, protein or both. Indeed, the membrane model we have espoused since 1966 [35] explicitly predicts linked and reciprocal configurational changes among penetrating membrane proteins and the components of abutting phospholipid boundary layers [36].

The X-ray experiments of Gottlieb and Eanes [24] on hydrated erythrocyte membrane lipids, depleted of cholesterol to varying extents, show that with 6 mol % of cholesterol, crystal (gel) and liquid-crystal states can coexist between +2 °C and +20 °C, although liquid-crystal domains predominate already at −10 °C, and at higher cholesterol proportions only the liquid-crystalline state is detected even at −20 °C. Concordant information has been reported by Jackson et al. [37] who found no calorimetrically detectable phase transition in hydrated membrane lipids unless 81 % of the cholesterol was removed. The latter preparations yielded a very broad transition (5–45 °C) centered at 25 °C.

In pure and mixed lipids, discontinuities of $[I_{\approx 2880}/I_{2850}]$ occur during crystal $\rightleftarrows$ liquid-crystal transition of phospholipid acyl chains, but these discontinuities are sharp only at low proportions of cholesterol [4, 8, 31]. One might thus ascribe the discontinuity in $[I_{\approx 2880}/I_{2850}]$ vs. temperature near 17 °C (corrected temperature) to a crystal $\rightleftarrows$ liquid-crystal transition in a region of low cholesterol content ($\leq$ 6 mol %), corresponding to that reported in [37]. The fact that this transition corresponds to the abrupt decrement of $[I_{1527}/I_{1158}]$ of membrane-bound β-carotene would fit the suggestion that a low-cholesterol region is involved since, earlier studies [2] indicate that β-carotene is excluded from cholesterol-rich domains. Similarly one might well attribute the broader steps in $[I_{\approx 2880}/I_{2850}]$ and $[I_{\approx 2932}/I_{2850}]$ to crystal $\rightleftarrows$ liquid crystal transition in domains of higher cholesterol content. However, other thermally-induced rearrangements of lipid architecture can also be expected to produce sharp discontinuities in Raman scattering.

Unfortunately, the contribution of amino acid side chains of membrane on the observed thermotropism cannot now be clearly assessed. There is no calorimetric evidence for thermotropic erythrocyte membrane protein transitions below 40 °C [23, 37] and we have found no discernible temperature sensitivity below 20 °C in the conformationally sensitive Amide III region [31]. In addition, proton magnetic resonance studies [38] show no alterations in the mobilities of erythrocyte membrane proteins below 40 °C, in accord with enzyme inactivation experiments [37].

It is known, however, that some proteins exhibit cooperative, reversible, thermally-induced transitions under unusual conditions, low pH in particular [39]. These occur near 20 °C, but not at very low temperatures. It is not inconceivable that membrane proteins may, at neutral pH behave as do soluble proteins at acid pH. It is also possible that Raman spectroscopy can reveal thermotropic structural vibrations that are not detected by other methods. Comparisons of the behavior of membranes with aqueous dispersions of their lipids [24, 28, 29] provide no resolution to these dilemmas, since even the simplest lipid cholesterol systems yield very diffuse thermotropic responses [4, 8].

Balancing the evidence, the simplest, but not exclusive interpretation of the data is that the observed transitions represent structural alterations of membrane lipids proceeding in lipid domains and/or lipid-protein complexes. We anticipate that resolution of the physical origins of the spectroscopic changes, will provide clues as to the mechanisms involved.

Third, even if the thermotropic responses described herein represent the behavior only of membrane phospholipids, we cannot now say how much lipid is involved in each of the several transitions described. Indeed, we cannot exclude the possibility that lipid state transitions occur at temperatures not yet explored by Raman spectroscopy (e.g. above 35 °C, where important protein changes are detected by measuring paramagnetic quenching of protein fluorescence [32]). However, it is known that lipid transitions can occur well above the temperature expected from the unsaturated phospholipids prevailing in erythrocyte membranes, due to the influence of hydrophobic [7] and/or ionic [13] protein-lipid interactions, as well as the possible ionic influence of divalent cations [40–42].

ACKNOWLEDGEMENTS

This work was supported by awards from the National Institutes of Health (CA 13061, CB 43922) and the American Cancer Society (DFHW).

REFERENCES

1 Wallach, D. F. H. and Verma, S. P. (1975) Biochim. Biophys. Acta 382, 542–551
2 Verma, S. P. and Wallach, D. F. H. (1975) Biochim. Biophys. Acta 401, 168–175
3 Lippert, J. L., Gorcayca, L. E. and Meiklejohn, G. (1975) Biochim. Biophys. Acta 382, 51–57
4 Verma, S. P., Wallach, D. F. H. and Schmidt-Ullrich, R. (1975) Biochim. Biophys. Acta 394, 633–645
5 Schmidt-Ullrich, R., Verma, S. P. and Wallach, D. F. H. (1976) Biochim. Biophys. Acta, in the press
6 Schmidt-Ullrich, R., Verma, S. P. and Wallach, D. F. H. (1975) Biochem. Biophys. Res. Commun. 67, 1062–1069
7 Verma, S. P. and Wallach, D. F. H. (1976) Biochim. Biophys. Acta, in the press.
8 Lippert, J. L. and Peticolas, W. L. (1971) Proc. Natl. Acad. Sci. U.S. 68, 1572–1576
9 Brown, K. G., Peticolas, W. L. and Brown, E. (1973) Biochem. Biophys. Res. Commun. 54, 358–366
10 Lippert, J. L. and Peticolas, W. L. (1972) Biochim. Biophys. Acta 282, 8–17
11 Schaufele, R. F. and Shimanouchi, T. (1967) J. Chem. Phys. 47, 3605–3610
12 Verma, S. P., Wallach, D. F. H. and Smith, I. C. P. (1974) Biochim. Biophys. Acta 345, 129–140
13 Papahadjopoulos, D., Moscarello, M., Eylar, G. H. and Isac, T. (1975) Biochim. Biophys. Acta 401, 317–355
14 Fairbanks, G., Steck, T. L. and Wallach, D. F. H. (1971) Biochemistry 10, 2606–2616
15 Harney, B. M. and Miller, M. A. (1970) Appl. Spectrosc. 2, 291–292
16 Savitsky, A. and Golay, M. J. E. (1964) Anal. Chem. 36, 1627–1639
17 Larsson, K. (1973) Chem. Phys. Lipids 10, 165–176
18 Larsson, K. and Rand, R. P. (1973) Biochim. Biophys. Acta 326, 245–258
19 Spiker, Jr., R. C. and Levin, I. W. (1975) Biochim. Biophys. Acta 388, 361–373
20 Tobin, M. C. (1971) Laser Raman Spectroscopy, pp. 29–31, 112, Wiley Interscience, New York
21 Eisenberg, D. P. and Kauzman (1969) The Structure of Water, pp. 121–127, 228–246, Oxford University Press, New York
22 Chapman, D. (1973) in Biological Membranes (Chapman, D. and Wallach, D. F. H., eds),. Vol. 2, pp. 91–144
23 Ladbrooke, B. D. and Chapman, D. (1969) Chem. Phys. Lipids 3, 304–307
24 Gottlieb, M. H. and Eanes, E. D. (1974) Biochim. Biophys. Acta 373, 519–522
25 Peters, R., Peters, J., Tews, K. H. and Bahr, W. (1974) Biochim. Biophys. Acta 367, 282–394
26 Wallach, D. F. H., Verma, S. P., Weidekamm, E. and Bieri, V. (1974) Biochim. Biophys. Acta 356, 68–81
27 Verma, S. P. and Wallach, D. F. H. (1975) Biochim. Biophys. Acta 382, 73–87
28 Zimmer, G. and Schirmer, H. (1974) Biochim. Biophys. Acta 345, 314–320
29 Zimmer, G. Schirmer, H. and Bastian, P. (1975) Biochim. Biophys. Acta 401, 244–255
30 Lacko, L., Wittke, B. and Geck, P. (1973) J. Cell. Physiol. 82, 213–218
31 Wallach, D. F. H., Bieri, V., Verma, S. P. and Schmidt-Ullrich, R. (1975) Proc. N. Y. Acad. Sci. 264, 142–160
32 Bieri, V. and Wallach, D. F. H. (1975) Biochim. Biophys. Acta 406, 415–423
33 Higgins, J. A., Florendo, N. T. and Barnett, R. B. (1973) J. Ultrastruct. Res. 42, 66–81
34 Siamwiza, N. M., Lord, R. C., Chen, M. C., Takamatsu, T., Harada, I., Matsura, H. and Shimansnichi, T. (1975) Biochemistry 14, 4870–4876
35 Wallach, D. F. H. and Zahler, H. P. (1966) Proc. Natl. Acad. Sci. U.S. 56, 1552–1559
36 Wallach, D. F. H. (1975) Membrane Molecular Biology of Neoplastic Cells, Chap. 11, pp. 483–497, Elsevier, Amsterdam
37 Jackson, W. M., Kostyla, J., Nordin, J. H. and Brandts, J. F. (1973) Biochemistry 12, 3662–3667
38 Sheetz, M. P. and Chan, S. I. (1972) Biochemistry 11, 548–555
39 Tanford, C. (1968) Adv. Protein Chem. 23, 121–282
40 Kimelberg, H. K. and Papahadjopoulos, D. (1974) J. Biol. Chem. 249, 1071–1080
41 Jacobson, K. and Papahadjopoulos, D. (1975) Biochemistry 14, 152–161
42 Träuble, H. and Eibl, H. (1974) Proc. Natl. Acad. Sci. U.S. 71, 214–219